Aspects of Artificial Photosynthesis. Energy Transfer in Cationic Surfactant Vesicles

Tadashi Nomura,[1] Jose R. Escabi-Perez,[2] Junzo Sunamoto,[3] and Janos H. Fendler*[2]

Contribution from the Department of Chemistry, Texas A&M University, College Station, Texas 77843, and the Department of Industrial Chemistry, Faculty of Engineering, Nagasaki University, Nagasaki 852, Japan. *Received July 16, 1979*

Abstract: Intermolecular Forster-type energy transfer has been observed in completely synthetic dioctadecyldimethylammonium chloride (DODAC) surfactant vesicles. The donor, lysopyrene, was localized in the hydrophobic bilayer of the vesicles. The acceptor, pyranine, having four negative charges, was attracted electrostatically to the outer surface of the positively charged DODAC vesicles. Depending on the concentration of pyranine, energy-transfer efficiencies up to 43% have been observed. Conversely, energy-transfer efficiencies in the absence of vesicles were less than 3%. Pyranine quenched the fluorescence intensity of DODAC intercalated lysopyrene. The second-order rate constant for the quenching, K_q, was calculated from a linear Stern-Volmer plot to be 6.2×10^{11} M^{-1} s^{-1}. This apparently high value is a consequence of an approximate 1000-fold acceptor concentration on the surface of the vesicles. The second-order rate constant for energy transfer, k'_{ET}, was calculated to be 4.9×10^{11} M^{-1} s^{-1}. Agreement between K_q and k'_{ET} values implies that energy transfer to pyranine is responsible entirely for quenching the lysopyrene fluorescence in DODAC vesicles. Resonication resulted in a redistribution of pyranine between the outer and inner surface of DODAC vesicles, which was manifested in changes in energy-transfer efficiencies. Dependencies of these changes were used to substantiate the proposed structure of the vesicles. The organizational ability of DODAC vesicles and its relevance to photochemical solar energy conversion are discussed.

Introduction

Completely synthetic surfactant vesicles are increasingly being utilized as membrane mimetic agents.[4] Sonic dispersal of long-chain dialkyldimethylammonium halides,[5-9] dialkyl phosphates,[10,11] sulfonates, carboxylates,[11] and even single-chain fatty acids[12] results in vesicle formation. Dioctadecyldimethylammonium chloride (DODAC) vesicles have been characterized most extensively. Well-sonicated DODAC gives fairly uniform single bilayer prolate ellipsoid vesicles having weight-averaged molecular weights of $(1-2) \times 10^7$.[13] DODAC vesicles are stable for weeks in the pH 2-12 range, have phase transition temperatures at 30.0 and at 36.2 °C, and are osmotically active and able to entrap apolar molecules.[4,9]

Surfactant vesicles have provided useful media for mimicking photosynthesis.[14-16] Photoionization,[14] electron transfer,[15] and efficient charge separation[16] have been demonstrated. Efficient electron transfer was observed from DODAC vesicle intercalated *N*-methylphenothiazine to photoexcited tris(2,2'-bipyridine)ruthenium^{2+} ion, anchored onto the surface of the vesicles by a long hydrocarbon chain.[16] The *N*-methylphenothiazine radicals formed were readily expelled both into the vesicle entrapped and into bulk water. Electrostatic repulsions between the cation radicals and the positively charged vesicle surface hindered undesirable charge recombinations. Parts of the *N*-methylphenothiazine cation radical which escaped from the vesicle into the bulk aqueous solution survived for extended periods (≫1 ms).[16] Interestingly, judicious addition of sodium chloride profoundly affected the lifetime of the cation radical and its partitioning between the aqueous inner core of the vesicles and bulk water.[16]

An important function of biological membranes is to organize molecules in their environments. Energy transfer in in vivo photosynthesis is largely dependent, for example, on the precise location of chlorophyll molecules in the chloroplast.[17] Efficient intermolecular energy transfer has been observed in DODAC vesicles in the present work. The donor, pyrene, was localized in the hydrophobic bilayer of the vesicles by a long hydrocarbon chain terminating in a polar choline group. The acceptor, pyranine, was electrostatically attracted to the outer charged surface of the DODAC vesicles. In the absence of vesicles (in alcohol), no energy transfer was observed. The obtained data provided additional confirmation of the proposed morphology[13] of DODAC vesicles.

Experimental Section

Preparation, purification, and characterization of dioctadecyldimethylammonium chloride (DODAC) have been described.[18,19] Trisodium 8-hydroxy-1,3,6-pyrenetrisulfonate (pyranine, Eastman)

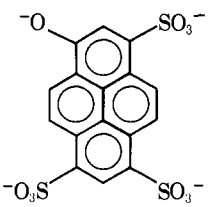

pyranine

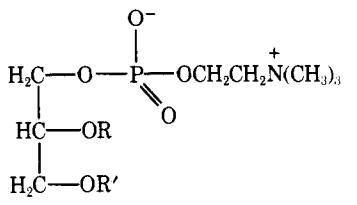

lysopyrene

R = H

R' = 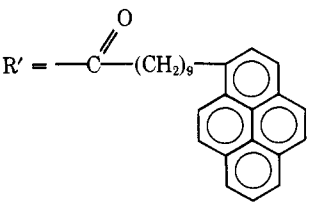

was purified by recrystallization from acetone-water (2:1 v/v, using charcoal. 2-Hydroxy-1-[ω-(1-pyreno)decanoyl]-*sn*-glycero-3-phosphatidylcholine (lysopyrene) was synthesized according to the method of Sunamoto.[20] Lysopyrene was purified by column chromatography (1.8-cm diameter, 70-cm long; silica gel, Wakogel C-100), using chloroform-methanol-water (65:25:4 v/v) as eluent, and by subsequent recrystallization from chloroform. The obtained white crystals melted at 206 °C dec. Infrared and ^{1}H NMR spectra confirmed the structure of lysopyrene. Anal. Cald for $C_{34}H_{46}O_7NP{\cdot}4H_2O$ (MV = 683.8): C, 59.7; H, 7.96; N, 2.05. Found: C, 59.3; H, 7.96; N, 2.08.

Surfactant vesicles were typically prepared as follows. A methanolic solution (70 μL) of 5.8×10^{-4} M lysopyrene was evaporated to dryness in a glass tube by a gentle stream of nitrogen gas. DODAC (12.0 mg) and 2.0 mL of doubly distilled water were put into the tube containing the thin film of lysopyrene. Dispersion was carried out by sonication for 15 min at 60 °C by means of the microprobe of a Bransonic 1510 sonifier set at 70 W. Titanium particles were removed by centrifugation for 15 min in a clinical centrifuge. The vesicle solution was passed through a Sephadex G-50 column. The vesicle

0002-7863/80/1502-1484$01.00/0

fraction, ca. 5.0 mL, was diluted to 15 mL, and its pH was adjusted to 8.75 by aqueous NaOH. Concentration of the vesicle-entrapped lysopyrene was determined spectrophotometrically, taking ϵ_{345nm} 3.5 $\times 10^4$ M^{-1} cm^{-1}. Pyranine was added externally; its concentration was also determined spectrophotometrically taking ϵ_{450nm} 2.7 $\times 10^5$ M^{-1} cm^{-1}.

Absorption spectra were taken on a Cary 118-C spectrophotometer. Steady-state fluorescence excitation and emission spectra were obtained on a SPEX Fluorolog spectrofluorimeter using the E/R mode. Front-face angle illumination was used to minimize inner filter effects. Generally, 2.5-mm slits and 10-nm band path were used. Fluorescence lifetimes were determined by means of a modified ORTEC 9200 single photon counting nanosecond time resolved fluorescence spectrometer with the output displayed on a multichannel analyzer.[21,22] Excitation wavelengths were selected by the use of appropriate filters (Ditric Optics, Inc.) having 5.0-nm half-height bandwidths. Fluorescence lifetimes were calculated on an on-line Digital PDP-11/10 computer using the method-of-moments program.[21] All spectral measurements were carried out at 26.0 ± 1.0 °C.

The vesicle samples in a sealed fluorescence cell were deaerated by purging with purified N_2 gas for 30 min. Methanol solutions were degassed on a high vacuum line by repeated freeze-pump-thaw cycles.

Results

Figure 1 shows the excitation and emission spectra of 6.9 $\times 10^{-7}$ M lysopyrene entrapped in DODAC vesicles (8.0 $\times 10^{-4}$ M stoichiometric surfactant concentration) at a bulk pH of 8.75. These spectra are similar to those in methanol. Apparently, lysopyrene is not a sensitive probe for reporting its microenvironment. Figure 1 also shows the excitation spectra of 9.13 $\times 10^{-3}$ M pyranine in the same DODAC vesicles. Both the excitation and the emission spectrum of pyranine are identical with those reported previously in phospholipid liposomes.[23] Ratios of excitation intensities of 450:400 nm, observed at an emission of 510 nm, of pyranine have been shown to be extremely sensitive to pH changes.[23] Using the published calibration curve[23] pyranine reported pH values exceeding 10 in the presence of DODAC vesicles, whose bulk pH had been adjusted to 8.75. This result is explicable in terms of increased local hydroxide ion concentration at the vesicle surface, resulting from a partial replacement of chloride by hydroxide ions on DODAC. Further implication of the apparent higher hydroxide concentration reported by the probe is that the completely ionized pyranine (having four negative charges) is localized at the charged surface of the vesicles.

Overlap of the emission spectrum of lysopyrene with the excitation spectrum of pyranine (Figure 1) indicates the possibility of Förster-type intermolecular energy transfer from lysopyrene to pyranine. Such energy transfer could be observed, in fact, in the presence of DODAC vesicles and is illustrated in Figure 1. Excitation at 345 nm (where direct energy absorption by pyranine is minimal) resulted in enhanced emission of pyranine at 510 nm, parallel with decreased lysopyrene emission at 380, 400, and 420 nm. Energy transfer was further substantiated by the observed nanosecond time resolved intensity changes at 510 nm, following excitation by 1-ns pulses of light at 334 nm. A typical buildup and decay of pyranine emission is shown in the insert in Figure 1.

Pyranine quenched the fluorescence intensity of DODAC-intercalated lysopyrene. Increasing concentrations of added pyranine resulted in decreased fluorescence of lysopyrene at 380 nm. The concentration quenching obeyed the Stern-Volmer relationship:

$$I_0/I - 1 = K_{sv}[\text{pyranine}] \qquad (1)$$

(where I_0 and I are emission intensities of lysopyrene in the absence and in the presence of pyranine and K_{sv} is the Stern-Volmer quenching constant) up to a stoichiometric pyranine concentration of 2.0 $\times 10^{-5}$ M. Beyond this concentration inner filter effects caused complications. Quenching data are

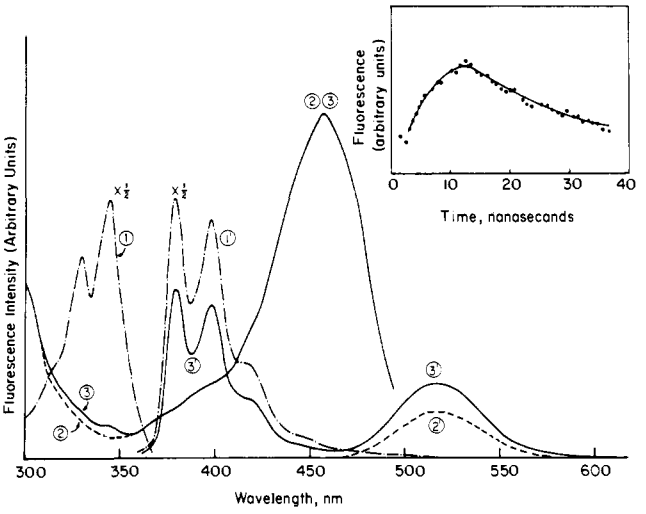

Figure 1. Excitation spectrum of 6.9 $\times 10^{-7}$ M lysopyrene intercalated in 8.0 $\times 10^{-4}$ M stoichiometric DODAC in the absence of energy transfer monitored at 380 nm (1, -·-·-); emission spectrum of 6.9 $\times 10^{-7}$ M lysopyrene intercalated in 8.0 $\times 10^{-4}$ M stoichiometric DODAC in the absence of energy transfer excited at 345 nm (1′, -·-·-); note that the intensity scales for spectra 1 and 1′ are reduced by a factor of ½. Excitation spectrum of 9.13 $\times 10^{-3}$ M pyranine in the presence of 8.0 $\times 10^{-4}$ M stoichiometric DODAC monitored at 510 nm (2, - - -); emission spectrum of 9.13 $\times 10^{-6}$ M pyranine in the presence of 8.0 $\times 10^{-4}$ M stoichiometric DODAC, excited at 345 nm (2′, - - -). Excitation spectrum of 6.9 $\times 10^{-7}$ M lysopyrene intercalated in 8.0 $\times 10^{-4}$ M stoichiometric DODAC in the presence of 9.13 $\times 10^{-6}$ M pyranine, monitored at 510 nm (3, ——). Emission spectrum of 6.9 $\times 10^{-7}$ M lysopyrene intercalated in 8.0 $\times 10^{-4}$ M stoichiometric DODAC in the presence of 9.13 $\times 10^{-6}$ M pyranine, excited at 345 nm (3′, ——). The insert shows the time-dependent buildup and decay of the pyranine fluorescence at 510 nm. Conditions are the same as that for 3′.

plotted according to eq 1 in Figure 2. The slope of this plot gives K_{sv} = 1.19 $\times 10^5$ M^{-1}. Using

$$K_{sv} = K_q\tau_0 \qquad (2)$$

(where τ_0 is the natural lifetime of lysopyrene, determined to be 190 ns) the apparent second-order rate constant for the quenching of the fluorescence of DODAC-intercalated lysopyrene by pyranine, concentrated on the surface of the vesicles, K_q, was calculated to be 6.2 $\times 10^{11}$ M^{-1} s^{-1}. This value is considerably higher than that associated with Förster-type quenching constants and is the consequence of using stoichiometric rather than "local" pyranine concentrations. Under the present experimental conditions, DODAC vesicles concentrate pyranine on their surfaces approximately 1000-fold.

Energy-transfer efficiencies, ET values, were calculated from the equation[24]

$$\text{ET} = A/A_D(F_D/F - 1) \qquad (3)$$

where A_D and A are absorbances at 345 nm in the presence and in the absence of lysopyrene; F_D and F are the relative emission intensities at 510 nm in the presence and in the absence of lysopyrene. Table I summarizes ET values at different pyranine concentrations. Fluorescence efficiencies of lysopyrene in DODAC vesicles in the presence of transfer, Φ_{LR}, were related to that of pyrene in cyclohexane, Φ_P, by the equation[24]

$$\Phi_{LP} = \Phi_P \frac{L_P\epsilon_P b_P\tau_P\Lambda_{LP}\eta_{LP}^2}{L_{LP}\epsilon_{LP}b_{LP}C_{LP}\Lambda_P\eta_P^2} \qquad (4)$$

where L is the lamp intensity, ϵ is the molar absorptivity at 345 nm, b is the path length of the cell in cm, C is the stoichiometric concentration of the substrate (lysopyrene or pyrene), Λ is the area under the emission peak 380 nm, and η is the refractive index of the solvent; subscripts LP and L refer to that of lyso-

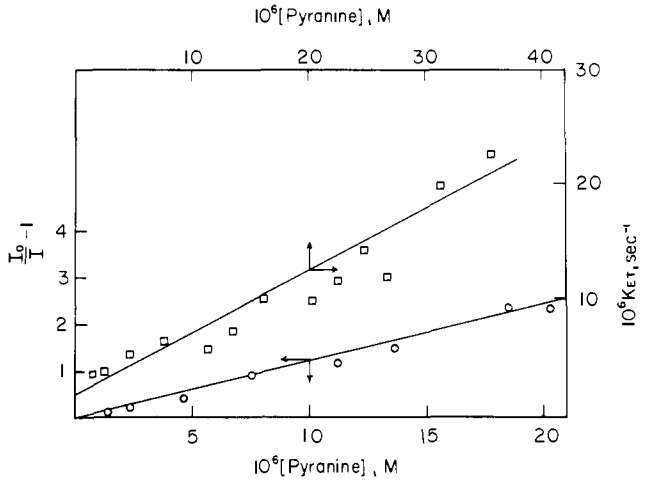

Figure 2. Stern-Volmer plot of lysopyrene quenching by pyranine in DODAC vesicles, according to eq 1 (○); a plot of energy-transfer rate constants against pyranine concentrations in DODAC vesicles (□).

pyrene in DODAC vesicles and to pyrene in cyclohexane, respectively. The following values were used: $\epsilon_{LP} = 3.5 \times 10^4$ M^{-1} cm^{-1}, $\epsilon_P = 4.9 \times 10^4$ M^{-1} cm^{-1},[24] $\eta_{LP} = 1.33$, $\eta_P = 1.44$, $\Phi_P = 0.65$,[24] $C_P = 3.2 \times 10^{-7}$ M. As expected, increasing concentrations of pyranine resulted in decreased lysopyrene fluorescence efficiencies (Table I).

Rate constants for the energy transfer, k_{ET}, were calculated from the equation

$$k_{ET} = \frac{ET}{\Phi_{LP}\tau_0} \tag{5}$$

k_{ET} values plotted linearly with stoichiometric pyranine concentrations (Figure 2). The shape of this plot gives an apparent second-order rate constant for energy transfer, $k'_{ET} = 4.9 \times 10^{11}$ M^{-1} s^{-1}. Once again, this value is very much higher than that found for intermolecular energy transfers in homogeneous solutions, and is a consequence of greatly enhanced pyranine concentrations at the vesicle surface. More importantly, the good agreement between K_q and k'_{ET} values implies that energy transfer to pyranine is responsible entirely for quenching the lysopyrene fluorescence in DODAC vesicles.

Since pyranine was externally added to the already formed lysopyrene carrying DODAC vesicles it is expected to reside on the outer surface. Heating above the phase transition temperature (36 °C) or sonicating results in melting and reforming of the vesicles with the concomitant distribution of the quencher between the inner and the outer surfaces. Energy transfer and quantum efficiencies were indeed changed upon heating or sonicating the DODAC vesicles. Pertinent data are also included in Table I.

Significantly, less than 3% energy transfer was observed if the donor and the acceptor were dissolved in methanolic 0.206 M sodium methoxide. In these experiments the concentration of lysopyrene was kept at 8.0×10^{-7} M and that of pyrene varied between 4.4 and 26.0×10^{-6} M. Owing to inner filter effects, higher concentrations of pyranine could not be used. Fluorescence intensities of DODAC vesicle intercalated 8.9×10^{-7} M lysopyrene were not quenched by the addition of $(1\text{-}6) \times 10^{-4}$ M NaI or NaBr.

Discussion

The most significant result of the present work is the demonstration of the organizational ability of completely synthetic DODAC surfactant vesicles. Lysopyrene molecules are anchored at the inner and outer surface of the vesicles by their polar head groups, while the pyrene moieties of the probes are intercalated among the hydrophobic hydrocarbon chain of

Table I. Quantum and Energy Transfer Efficiencies of DODAC-Intercalated Lysopyrene as a Function of Added Pyranine[a]

10^6[pyranine], M	ET, %	Φ_{LP}[b]
1.38	38	0.535
2.38	36	0.491
4.60	43	0.422
7.47	39	0.313
11.20	30	0.273
13.60	34	0.241
16.00	36	0.172
20.40	33	0.173
22.40	28	0.126
24.60	23	0.084
26.80	13	0.062
31.20	20	0.053
35.60	15	0.035
11.20[c]	28	0.479
11.20[c,d]	39	0.313
18.50[c]	29	0.249
18.50[c,d]	42	0.187
24.50[c]	32	0.159
24.50[c,d]	27	0.121

[a] Stoichiometric lysopyrene concentration = 6.9×10^{-7} M, unless stated otherwise; stoichiometric DODAC concentration is 8.0×10^{-4} M. [b] Defined by eq 4. [c] Stoichiometric lysopyrene concentration is 9.4×10^{-7} M. [d] Following resonication, subsequent to the addition of pyranine.

DODAC. Under the present experimental conditions each vesicle contains less than six molecules of lysopyrene and is associated with up to 2800 molecules of pyranine. Although corresponding concentrations of donors (8.0×10^{-7} M) and acceptors ($(4\text{-}26) \times 10^{-6}$ M) are insufficient for energy transfer in homogeneous solutions, localization of them in the vesicles, themselves present at very low concentrations (1.4×10^{-8} M), renders this process efficient.

The observed intermolecular energy transfer from lysopyrene to pyranine, in DODAC vesicles, can be analyzed in terms of interchromophoric distances. The average distance between a donor and an acceptor, $\langle R \rangle$, is calculated from the Förster equation:[25]

$$k_{ET} = \frac{9(\ln 10)K^2}{128\pi^5 N\eta^4\langle R^6\rangle\tau_0} J \tag{6}$$

where K is the dipole-dipole orientation factor, N is Avogadro's number, η is the refractive index of the medium, and J is the overlap integral. Using the calculated values for k_{ET} (Table I) and those for the overlap integrals (not given), and assuming $K^2 = {}^2/_3$[26] and $\eta = 1.33$, allowed the assessment of $\langle R \rangle$ (Figure 3). The maximum average distance, at the lowest pyranine concentration, between the donor and acceptor is 60 Å. Increasing concentrations of added pyranine results in decreased $\langle R \rangle$ values. Inner filter effects precluded the extension of energy-transfer experiments to higher pyranine concentrations (vide supra). The shortest determined interchromophoric distance, 45 Å, can be considered to approximate half the thickness of a bilayer in a DODAC vesicle. This approximation should be compared with the value previously determined by low angle laser light scattering and photon correlation spectroscopy.[13] The results of this latter work indicated well-sonicated DODAC vesicles to be prolate ellipsoids with axes of 812 and 126 Å and bilayer thickness of 50 Å.[13] Taking these values, the surface area of a DODAC vesicle is calculated to be 1.0×10^6 Å^2. Further, taking into consideration charge repulsions, the average area of a pyranine molecule is estimated to be 400 Å^2. Accordingly, it takes 2.6×10^3 molecules of pyranine to cover completely the outside surface of a DODAC vesicle. At the present experimental condition, 8.0×10^{-4} M stoichiometric DODAC, the vesicle concentration is 1.0×10^{-8} M (av mol wt of a vesicle is $\sim 3.15 \times 10^6$).[13] Thus all the

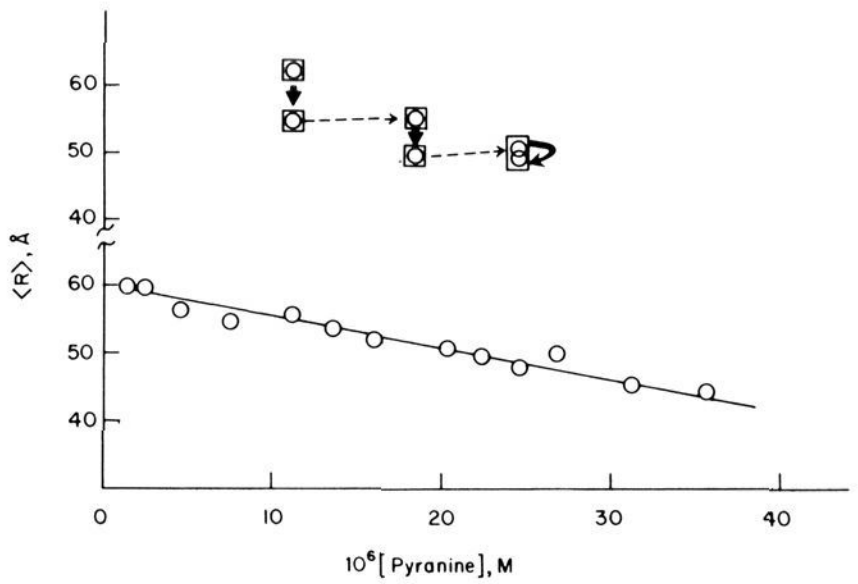

Figure 3. Lower portion: plot of $\langle R \rangle$ values, for the intermolecular energy transfer from DODAC-intercalated lysopyrene to pyranine (localized at the surface of the vesicles), against pyranine concentrations, according to eq 6. In the upper portion, the arrows indicate the effects of sonication at given pyranine concentrations.

available outer surface of the vesicles is expected to be covered at a stoichiometric pyranine concentration of 3.6×10^{-5} M.

The validity of these morphological approximations was tested by examining changes in energy-transfer efficiencies subsequent to resonicating the lysopyrene intercalated pyranine-carrying DODAC vesicles (Table I). The upper part of Figure 3 illustrates the obtained results in terms of $\langle R \rangle$ values. The average interchromophoric distance between donor and acceptor molecules is seen to decrease from 62 to 55 Å subsequent to resonication in the presence of 11.2×10^{-6} M pyranine. The corresponding decrease at 18.5×10^{-6} M pyranine is somewhat smaller (from 55 to 50 Å). At a stoichiometric pyranine concentration of 24.6×10^{-6} M or higher, resonication did not alter energy-transfer efficiencies. These results are rationalized by assuming that pyranine adds to the outer surface of the vesicles and does not penetrate across their bilayers. The bulkiness and charge density of pyranine render this interpretation reasonable. Resonication opens up and reseals the vesicles and hence it results in a distribution of pyranine between the inner and outer surface. At lower pyranine concentrations the consequence of the redistribution is a statistical decrease of the average interchromophoric distance between the donors and acceptors. At 24.6×10^{-6} M pyranine concentration, the outer surface of the vesicles is covered to such an extent that redistribution does not lower further the effective interchromophoric distances. Bearing in mind the approximations involved, this value is considered to be in a good agreement with that calculated for the concentration of pyranine needed for covering the surface of all available DODAC vesicles (3.6×10^{-5} M). These results lend credence to the proposed shape and size of DODAC vesicles. Figure 4 schematically shows a lysopyrene-containing DODAC vesicle in the presence of added pyranine.

Table II. Experimental and Theoretical Quenching Parameters[a]

10^6[pyranine], M	a_1[b]	I/I_0 calcd[c]	I/I_0 found
1.38	0.294	0.87	0.87
2.31	0.493	0.79	0.82
4.60	0.981	0.64	0.71
7.41	1.590	0.50	0.53
11.20	2.400	0.38	0.46
13.50	2.910	0.33	0.40
16.00	3.410	0.28	0.30
20.40	4.340	0.23	0.30

[a] Stoichiometric lysopyrene concentration = 9.4×10^{-7} M; stoichiometric DODAC concentration = 8.0×10^{-4} M. [b] Average number of acceptors within $\sqrt{2.6}R_0$ of donor, as defined by eq 7. [c] Calculated by means of eq 7 as described in the Discussion.

Equations have been derived to predict the quenching of fluorescence due to energy transfer between randomly distributed donors and acceptors in planar monolayers[27] and lipid vesicles.[28] Interestingly, fractional fluorescence intensities, I/I_0 values, were accurately predicted both for planar bilayers and spherical vesicles.[28] This was an apparent consequence of the insensitivity of K^2 to vesicle curvatures. An agreement between predicted and calculated I/I_0 values for energy-transfer quenching in DODAC vesicles would, therefore, justify the use of $K^2 = \frac{2}{3}$, originally derived for spherical particles having rapid isotropic reorientation during the donor emission lifetime.[29,30] I/I_0 values were calculated by means of the equation[29]

$$I/I_0 = \frac{1 - e^{a_1}}{a_1} \tag{7}$$

where a_1 is the average number of acceptors within R_d distance of a donor. Letting the average number of acceptors be $\bar{n}$ per unit area, $a_1 = \pi \bar{n} R_d^2$. The average number of acceptors per Å^2 was calculated by multiplying one-half of the ratio of pyranine to DODAC molecules by the area occupied by one DODAC molecule. An area of 71.7 Å^2 was taken for each DODAC molecule: R_d, an adjustable parameter, was taken to be $\sqrt{2.6}R_0$,[28] where R_0, the distance at which the rate constant for energy transfer equals the rate constant for deactivation of the excited state in the absence of acceptors, was calculated to be 38.7 Å. It is seen in Table II that eq 7 predicts well the quenching of DODAC-entrapped lysopyrene

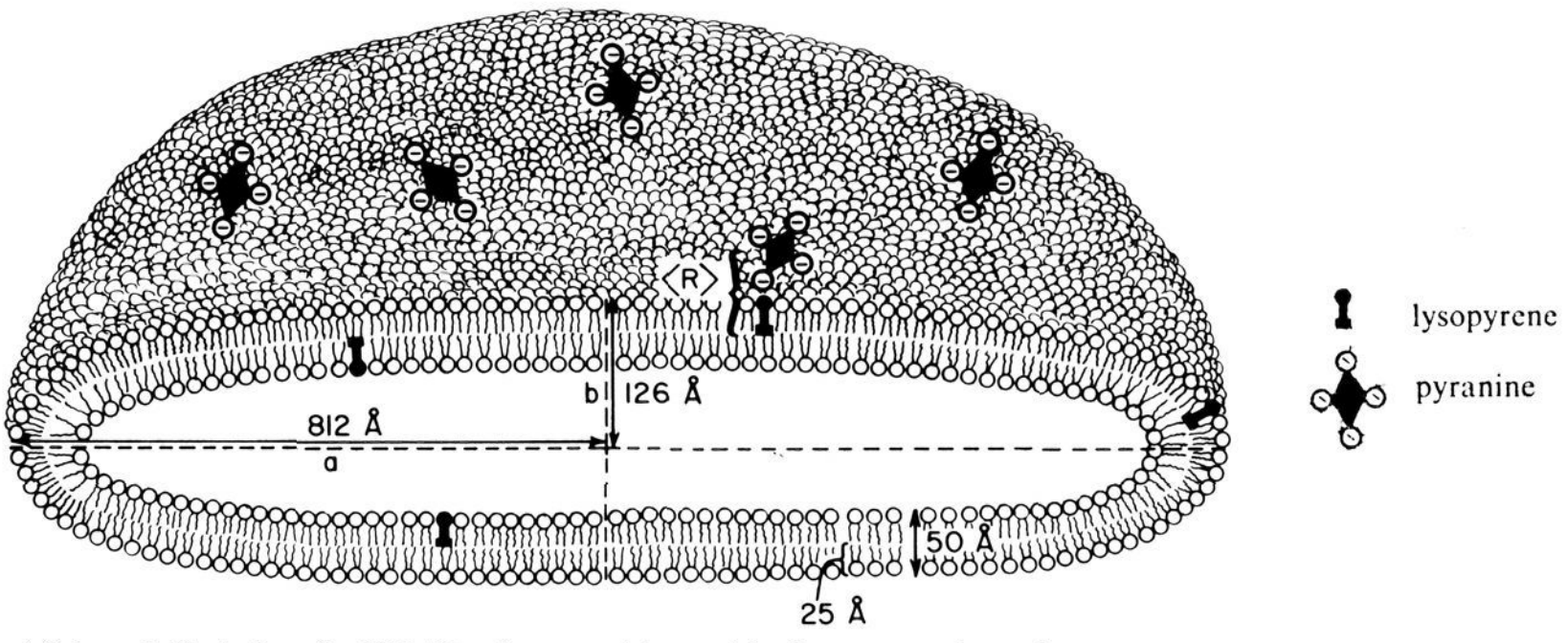

Figure 4. Schematic illustration of a DODAC surfactant vesicle containing lysopyrene and pyranine.

fluorescence intensities by pyranine. These data lend credence, therefore, to the assessment of average intermolecular distances from the rate constants for energy transfer.

The enhanced energy transfer reported in the present work is entirely due to a Förster-type mechanism. The lack of observable quenching of vesicle-entrapped donor fluorescence by added iodide or bromide ions (see above) obviates the possibility of energy transfer by the encountering of donor and acceptor molecules at the vesicle surface. The acceptable correlation between the observed and calculated fluorescence quenching as well as the insignificant energy transfer in methanol is also in accord with the proposed Förster-type mechanism. Orientation of dipoles at appropriate distances and compartmentalization of donor and acceptor molecules are responsible for the enhanced energy transfer.

Taken together, the present work justifies the use of completely synthetic surfactant vesicles as membrane models. They possess all the desirable functions of the more complex liposomes, without their chemical instability. Most importantly, they can be readily manipulated and functionalized. These properties will find increasing use in photochemical solar energy conversions.

Acknowledgments. Support of the National Science Foundation and the Robert A. Welch Foundation is gratefully acknowledged.

References and Notes

(1) On leave from Nagasaki University.
(2) Texas A&M University.
(3) Nagasaki University.
(4) Fendler, J. H. *Acc. Chem. Res.*, **1980**, *13*, 7.
(5) Kunitake, K.; Okahata, Y.; Tamaki, K.; Takayanagi, M.; Kumamaru, F. *Chem. Lett.* **1977**, 387.
(6) Kunitake, T.; Okahata, Y. *J. Am. Chem. Soc.* **1977**, *99*, 3890.
(7) Kunitake, T.; Okahata, Y. *Chem. Lett.* **1977**, 1337.
(8) Deguchi, K.; Mino, J. *J. Colloid Interface Sci.* **1978**, *65*, 155.
(9) Tran, C. D.; Klahn, P. L.; Romero, A.; Fendler, J. H. *J. Am. Chem. Soc.* **1978**, *100*, 1622.
(10) Kunitake, T.; Okahata, Y. *Bull. Chem. Soc. Jpn.* **1978**, *51*, 1877.
(11) Mortara, R. A.; Quina, F. H.; Chaimovich, H. *Biochem. Biophys. Res. Commun.* **1978**, *81*, 1080.
(12) Hargreaves, R.; Deamer, D. W. *Biochemistry* **1978**, *17*, 3759.
(13) Herrmann, U.; Fendler, J. H. *Chem. Phys. Lett.* **1979**, *64*, 270.
(14) Escabi-Perez, J. R.; Romero, A.; Lukac, S.; Fendler, J. H. *J. Am. Chem. Soc.* **1979**, *101*, 2231.
(15) Infelta, P. P.; Fendler, J. H. *Photochem. Photobiol.*, in press.
(16) Infelta, P. P.; Grätzel, M.; Fendler, J. H. *J. Am. Chem. Soc.*, preceding paper in this issue.
(17) Porter, G. *Proc. R. Soc. London, Ser. A* **1978**, *362*, 281. *Pure Appl. Chem.* **1978**, *50*, 263.
(18) Lim, Y. Y.; Fendler, J. H. *J. Am. Chem. Soc.* **1979**, *101*, 4023.
(19) Kano, K.; Romero, A.; Djermouni, B.; Ache, H. J.; Fendler, J. H. *J. Am. Chem. Soc.* **1979**, *101*, 4030.
(20) Nomura, T.; Kondo, X.; Sunamoto, J., submitted for publication.
(21) Sheih, P. S. Dissertation, Texas A&M University, 1976.
(22) Correll, G. D.; Cheser, R. N., III; Nome, F.; Fendler, J. H. *J. Am. Chem. Soc.* **1978**, *100*, 1254.
(23) Kano, K.; Fendler, J. H. *Biochim. Biophys. Acta* **1978**, *509*, 289.
(24) Parker, C. A. "Photoluminescence of Solutions"; Elsevier: Amsterdam, 1968. Birks, J. B. "Photophysics of Aromatic Molecules"; Wiley: New York, 1970.
(25) Förster, Th. In "Modern Quantum Chemistry", Sinanoglu, Ed.; Academic Press: New York, 1965; Part III, p 93.
(26) Conrad, R. H.; Brand, L. *Biochemistry* **1968**, *7*, 777.
(27) Tweet, A. G.; Bellamy, W. G.; Gaines, G. L. *J. Chem. Phys.* **1964**, *41*, 2068.
(28) Estep, T. N.; Thompson, T. E. *Biophys. J.* **1979**, *26*, 195.
(29) Ware, W. R. *J. Phys. Chem.* **1961**, *83*, 4374.
(30) Cogan, U.; Shinitzky, M.; Weber, G.; Nishida, F. *Biochemistry* **1973**, *12*, 521.

Semiconductor Electrodes. 27. The p- and n-GaAs–*N,N'*-Dimethyl-4,4'-bipyridinium System. Enhancement of Hydrogen Evolution on p-GaAs and Stabilization of n-GaAs Electrodes

Fu-Ren F. Fan, Benjamin Reichman, and Allen J. Bard*

Contribution from the Department of Chemistry, The University of Texas at Austin, Austin, Texas 78712. *Received August 27, 1979*

Abstract: The photoelectrochemical (PEC) behavior of *N,N'*-dimethyl-4,4'-bipyridinium (methylviologen, MV^{2+}) at p- and n-type GaAs electrodes in aqueous solutions was studied. The reduction of MV^{2+} at irradiated p-GaAs occurs at potentials ~450 mV less negative than those found at a Pt electrode. The catalyzed reaction of the photogenerated $MV^{+}\cdot$ with water to produce hydrogen by irradiation of p-GaAs was demonstrated and the use of the MV system as an intermediate in the photoassisted generation of hydrogen at semiconductors with high hydrogen overpotentials suggested. The photooxidation of $MV^{+}\cdot$ at n-GaAs occurred at potentials ~0.8 V less positive to those where the oxidation takes place at Pt. PEC cells of the form n-GaAs or p-GaAs/MV^{2+}, $MV^{+}\cdot$/M were also constructed.

Introduction

Attempts to promote the photodecomposition of water at semiconductor electrodes are based on the reduction of protons to hydrogen at p-type and the oxidation of water to oxygen at n-type materials. In the design of such systems difficulties arise from instability of the semiconductor electrodes themselves under irradiation and low rates of hydrogen or oxygen evolution at the semiconductor surfaces. The large band gap n-type semiconductors which are stable and provide the needed overpotential for oxygen evolution, e.g., TiO_2[1] or $SrTiO_3$,[2] do not utilize solar energy very efficiently. The use of p-type materials in such cells has been less studied. Generally the efficiencies of p-type materials are low and they are apparently poor photocathodes for hydrogen evolution.[3]

We recently discussed the behavior of p-GaAs in aqueous solutions containing a number of redox couples and showed that stable operation of photoelectrochemical (PEC) cells for the conversion of radiant to electrical energy was possible.[4] A number of studies have described the production of hydrogen by reaction of the radical cation of *N,N'*-dimethyl-4,4'-bipyridinium (also known as methylviologen, MV^{2+}) with protons in the presence of a suitable catalyst (e.g., PtO_2).[5] In such

0002-7863/80/1502-1488$01.00/0